# SQUARE FILLET OCTAGONAL PHOTONIC CRYSTAL FIBER AS DISPERSION COMPENSATING FIBER USING THE GOLDEN RATIO

Fatin Nadirah<sup>a</sup>, Abdul Mu'iz Maidi<sup>a</sup>, Pg Emeroylariffion Abas<sup>a</sup>, Norazanita Shamsuddin<sup>a</sup>, and Feroza Begum<sup>a,\*</sup> <sup>a</sup>Faculty of Integrated Technologies, Universiti Brunei Darussalam, Bandar Seri Begawan, Brunei Darussalam

#### **Abstract**

This paper presents a simple square fillet octagonal lattice photonic crystal fibre (PCF) having 5 layers of air hole rings. Guiding properties of the PCF are investigated using finite element method (FEM) with perfectly matched layer (PML) as its boundary. Through analysis, it is possible to attain a negative chromatic dispersion of -377 ps/(nm.km) and low confinement loss of 0.00421dB/km at  $1.55~\mu m$  wavelength by selecting optimum parameters for the PCF. Additionally, the PCF is able to cover the E+S+C+L+U and partial O (1320 - 1700 nm) wavelength bands, with relative dispersion slope (RDS) value of  $0.0036nm^{-1}$ , similar to that of a single mode fibre. This makes the proposed PCF a potential candidate for a dispersion compensating fibre.

Keywords: chromatic dispersion, octagonal photonic crystal fibre, confinement loss, dispersion compensating fibre, effective area

## 1.0 INTRODUCTION

Photonic crystal fibres (PCFs) [1], unlike conventional fibres, consist of silica with an array of microscopic air holes in the cladding that run along the length of the fibre [2]. One unique attribute of PCFs is their design flexibility, whereby several parameters, including lattice pitch, design, diameter and number of air holes can be modified [3], depending on the application requirements of the fibre. In turn, remarkable optical properties, such as high negative dispersion, low confinement loss, single-mode, high birefringence and high nonlinearity can be achieved. Because of this, PCFs are potentially applicable in numerous optical applications, including dispersion compensation [4], supercontinuum generation [5] and in sensing applications [6].

Chromatic dispersion is a common phenomenon found in single-mode fibres (SMFs), whereby different light frequencies travelling along together arrive at different times, resulting in pulse broadening. This is a huge drawback in long-distance optical fibre communication system, which has to transport large bits of data. One way of counteracting this problem is by introducing dispersion compensating fibres (DCFs) with high negative dispersion to the link, to compensate for the positive dispersion caused by the SMF over a wide range of wavelength [4]. PCFs are suitable for this application, since high negative dispersion can be achieved by manipulating their structures. However, advancements in technology have resulted in extra requirements, with low confinement loss and ease of fabrication as additional parameters that should be considered.

Many PCF structures, designed to function as DCFs, have been reported in the literature, focusing on high negative dispersion and low confinement loss [7-11]. Lee et al. [7] proposed a square PCF with double-hole assisted core, which produces a negative dispersion of -150 ps/(nm.km) and low confinement loss over the E+S+C+L+U and partial O (1320 - 1700 nm) wavelength bands. Meanwhile, Hasan et al. [8] proposed a hybrid PCF with negative dispersion between -242.22 ps/(nm.km) and -762.6 ps/(nm.km) at the 1.30  $\mu$ m to 1.65  $\mu$ m wavelength range, having confinement loss in the order  $10^{-3}$ dB/km, whilst Mia et al. [9] proposed a heptagonal PCF core and cladding with -940 ps/(nm.km) dispersion and confinement loss of  $10^{-5}$  dB/km. Although both designs [8, 9] have demonstrated high negative dispersion values and low confinement losses, they have complicated structures with varying air hole sizes, making the fabrication process difficult. Modified octagonal PCF was proposed by Ahmad et al. [10], exhibiting a dispersion value of -511 ps/(nm.km) at 1.55  $\mu$ m wavelength and high confinement loss in the order of  $10^{-2}$  dB/km. Bala et al. [11] introduced a triangular lattice PCF with a very high negative dispersion of -9486 ps/(nm.km), however, no confinement loss has been reported.

The golden ratio, represented by the Greek alphabet phi  $(\phi)$ , is a mathematical ratio of value 1.618. Being used throughout nature, from shells to flowers, it has also been used in well-known architectures such as the Parthenon in Athens and Khufu's Pyramid of Egypt [12], both of which are still standing strong to this day. Although this principle has been used for centuries, the study of the golden ratio in PCFs is still relatively new. The principle of the golden ratio has been used to design PCFs to take advantage of their simple structure [13]; albeit not for the application of DCF. A simple hexagonal photonic crystal fibre using the golden ratio principle has been presented [13], producing a near-zero dispersion and low confinement loss, for data communication applications. To take advantage of the simple structure to facilitate fabrication, the golden ratio is used in this study, by fixing the ratio of pitch to air hole diameter, to the golden ratio value; in order to strengthen the structure of the PCF, whilst still maintaining a simple design.

This paper presents an octagonal PCF with 5 layers of square filleted air hole rings using the golden ratio principle. At optimum  $\Lambda = 1.0~\mu m$ , the proposed PCF achieves high negative chromatic dispersion of -369~ps/(nm.km) and low confinement loss of 0.0042 dB/km. Effective area, nonlinearity and relative dispersion slope have also been investigated.

### 2.0 GEOMETRY OF THE PROPOSED DESIGN

A cross-section of the proposed PCF is given in Figure 1, showing an octagonal lattice structure with air holes in the form of square fillets. Length of the square fillets air holes is given by I, while  $\Lambda$  and  $\Lambda_1$  represent the distance between adjacent air holes from the same ring and different rings, also referred to as pitch, respectively. The two pitches are related by  $\Lambda = 0.765\Lambda_1$ . The structure of the proposed PCF is based on fixing the ratio of pitch  $\Lambda$  to the length of the square fillet air holes, I, to be equal to the golden ratio:

Based on equation (1), varying pitch  $\Lambda$  varies the length I of the air hole and vice versa, to maintain the golden ratio rule. Both core and cladding material of the proposed PCF are made of silica with refractive index of 1.45, whilst the air holes have a refractive index of 1. The PCF structure is surrounded by a perfectly matched layer (PML) [3], absorbing any light rays passing from the core to the cladding, by suppressing any unwanted boundary reflection from the electromagnetic wave. Using a fine mesh type, the total number of elements is 16578, of which 8322 are boundary elements and 968 are vertex elements.

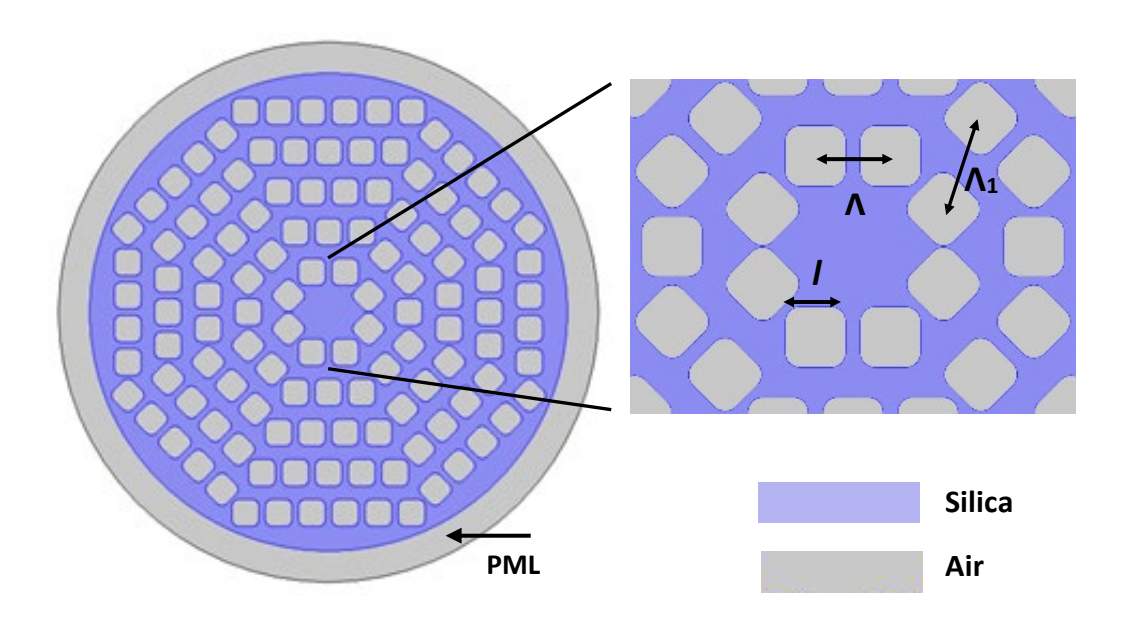


Figure 1: Cross-sectional structure of the proposed PCF

## 3.0 ANALYSIS METHOD

To simulate and investigate the properties of the proposed PCF, a full vector Finite Element method (FEM) was used with a cylindrical PML as the boundary condition of the PCF. The Sellmeier equation was used to determine the effective refractive index,  $n_{eff}$ , which is given by [14, 15]:

$$n_{\text{eff}} = \sqrt{1 + \frac{B_1 \lambda^2}{\lambda^2 - C_1} + \frac{B_2 \lambda^2}{\lambda^2 - C_2} + \frac{B_3 \lambda^2}{\lambda^2 - C_3}}$$
 (2)

where  $\lambda$  is the wavelength, and  $B_1$ ,  $B_2$ ,  $B_3$ ,  $C_1$ ,  $C_2$  and  $C_3$  are the Sellmeier coefficients. Effective refractive index has no unit and varies for each and every wavelength according to equation (2). Other properties of the PCF can then be calculated after determining the effective refractive index,  $n_{\text{eff}}$  of the PCF.

Several optical properties of the proposed PCF can be found using equations (3)-(6) [14-19]. Chromatic dispersion *D*, with unit ps/(nm.km) is given by [14, 15]:

$$D(\lambda) = -\frac{\lambda}{c} \frac{d^2 \operatorname{Re}[n_{\text{eff}}]}{d\lambda^2}$$
 (3)

where  $Re[n_{eff}]$  and c represent the real part of the effective refractive index,  $n_{eff}$ , and the speed of light, respectively.

Confinement loss,  $L_c$  with unit dB/km, is given by [14, 15]:

$$L_c = 8.686 \times k_0 \text{Im}[n_{\text{eff}}] \tag{4}$$

where  $k_0=\frac{2\pi}{\lambda}$  is the free space wave number and  ${\rm Im}[n_{\rm eff}]$  is the imaginary part of the effective refractive index.  $n_{\rm eff}$ .

Effective area  $A_{eff}$  with unit  $\mu m^2$  is given by [14, 15]:

$$A_{\text{eff}} = \frac{(\iint |\mathbf{E}^2| \ dxdy)^2}{\iint |\mathbf{E}|^4 \ dxdy} \tag{5}$$

where E is the amplitude of the transverse electric field propagating inside the PCF.

The nonlinearity coefficient  $\gamma$  with unit W<sup>-1</sup>km<sup>-1</sup> is calculated using [16, 17]:

$$\gamma = \frac{2\pi}{\lambda} \frac{n_2}{A_{\text{eff}}} \times 10^3 \tag{6}$$

where  $n_2 = 3.0 \times 10^{-20}$  m<sup>2</sup>/W is the non-linear refractive index of pure silica material [16].

Other important properties that need to be investigated to qualify the proposed PCF as a candidate for dispersion-compensating fibre are total residual dispersion,  $D_T$  and relative dispersion slope, RDS. These properties are calculated as follows [18, 19]:

$$D_T = D_{\text{SMF}} \cdot L_{\text{SMF}} + D_{\text{DCF}} \cdot S_{\text{DCF}} \tag{7}$$

$$RDS = \frac{S_{SMF}}{D_{SMF}} = \frac{S_{DCF}}{D_{DCF}}$$
 (8)

where  $D_{\rm SMF}$  and  $D_{\rm DCF}$  are dispersion coefficients of single-mode fiber and dispersion compensating fibre, respectively, with  $D_{\rm DCF}$  derived using equation (3).  $L_{\rm SMF}$  and  $L_{\rm DCF}$  are lengths of single mode fibre and dispersion compensating fibre, respectively.  $L_{\rm SMF}$  is taken to be 40 km, the standard length for analysis of dispersion compensating fibre whilst  $L_{\rm DCF}$  is chosen such that total residual dispersion equals to zero at 1.55  $\mu$ m wavelength.

Dispersion slopes of single-mode fibre and dispersion compensating fibre are denoted by S<sub>SMF</sub> and S<sub>DCF</sub>, respectively and can be found by the equation below:

$$S_{SMF}$$
 or  $S_{DCF} = \frac{dD(\lambda)}{d(\lambda)}$  (9)

## 4.0 SIMULATION RESULTS

Simulation results were based on four different pitch ( $\Lambda$ ) values at 0.05  $\mu$ m intervals: 0.95  $\mu$ m, 1.0  $\mu$ m, 1.05  $\mu$ m and 1.1  $\mu$ m. The effective refractive index of the proposed PCF is obtained for different  $\Lambda$  and wavelength, used as a basis for analysis, as shown in Figure 2. It can be seen that the effective refractive index,  $n_{\rm eff}$ , decreases as wavelength increases, with low  $\Lambda$  giving a lower effective refractive index. This is in accordance with equation (1), whereby the effective refractive index should decrease with increasing wavelength. At the lowest  $\Lambda$ , the effective refractive index,  $n_{\rm eff}$  ranges from 1.338 at 1.2  $\mu$ m wavelength to 1.271 at 1.7  $\mu$ m wavelength, while at the highest  $\Lambda$ , the effective refractive index,  $n_{\rm eff}$  ranges from 1.361 to 1.300 from the 1.2  $\mu$ m to 1.7  $\mu$ m wavelength range. In the other way, we can say that lower  $\Lambda$  results in less silica in the cladding, which in turn decreases the effective refractive index,  $n_{\rm eff}$ . On the other hand, higher  $\Lambda$  results in more silica in the cladding, which in turn increases the effective refractive index,  $n_{\rm eff}$ .

Negative dispersion is one of the main properties of PCF, which determines its applicability as a DCF. Since chromatic dispersion in SMF can cause accumulation of positive dispersion in the links, the proposed PCF needs to exhibit as high negative dispersion as possible for a wide range of wavelengths. As can be seen in Figure 3, negative dispersion increases with wavelength; with low  $\Lambda$  giving higher negative dispersion. At 1.55  $\mu$ m wavelength,  $\Lambda$  = 0.95  $\mu$ m exhibits the highest negative dispersion value of - 517 ps/(nm.km), followed by -377 ps/(nm.km), -261 ps/(nm.km) and -166 ps/(nm.km) for  $\Lambda$  = 1.0  $\mu$ m,  $\Lambda$  = 1.05  $\mu$ m and  $\Lambda$  = 1.1  $\mu$ m, respectively.

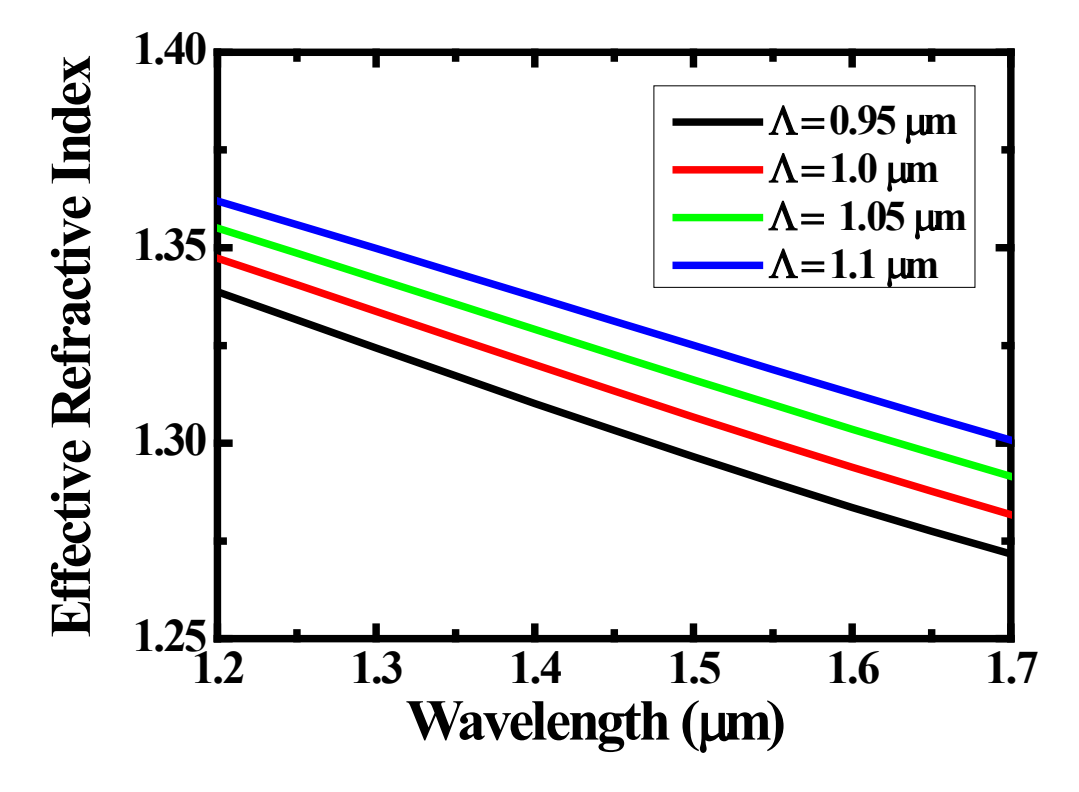


Figure 2: The effect of different values of  $\Lambda$  on the relationship between effective refractive index and wavelength.

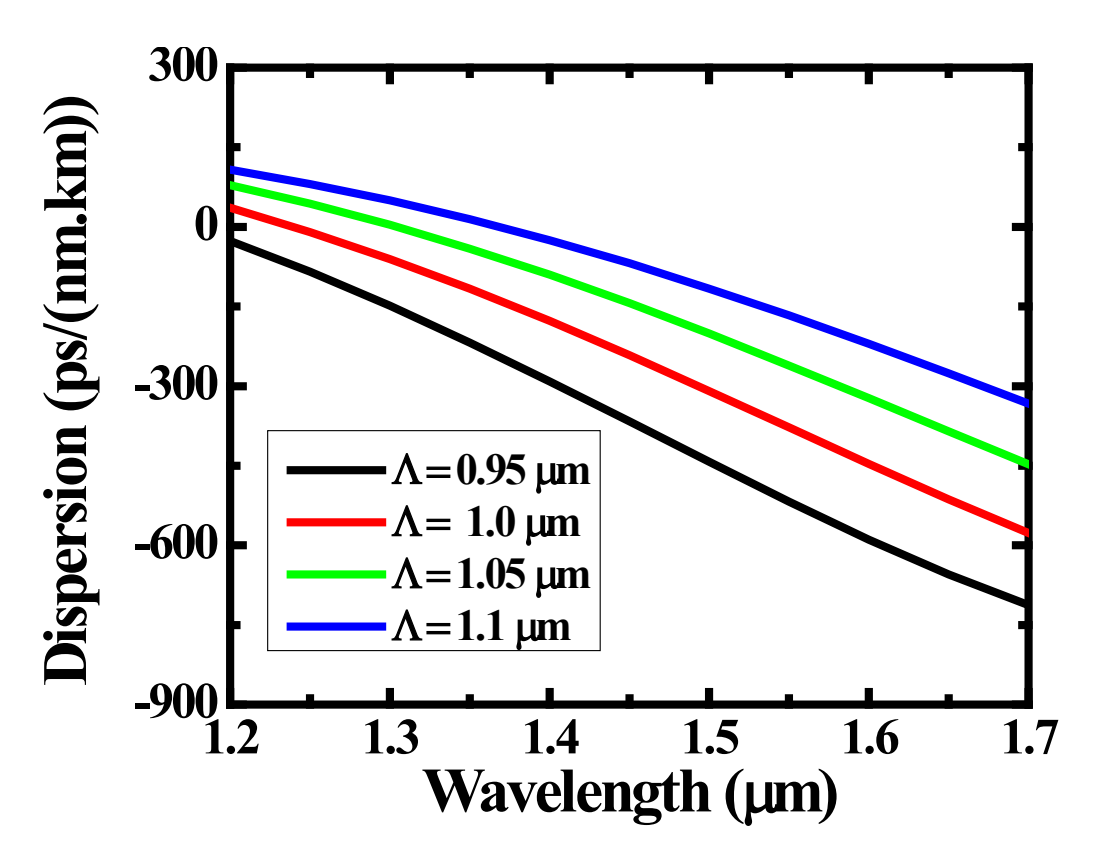
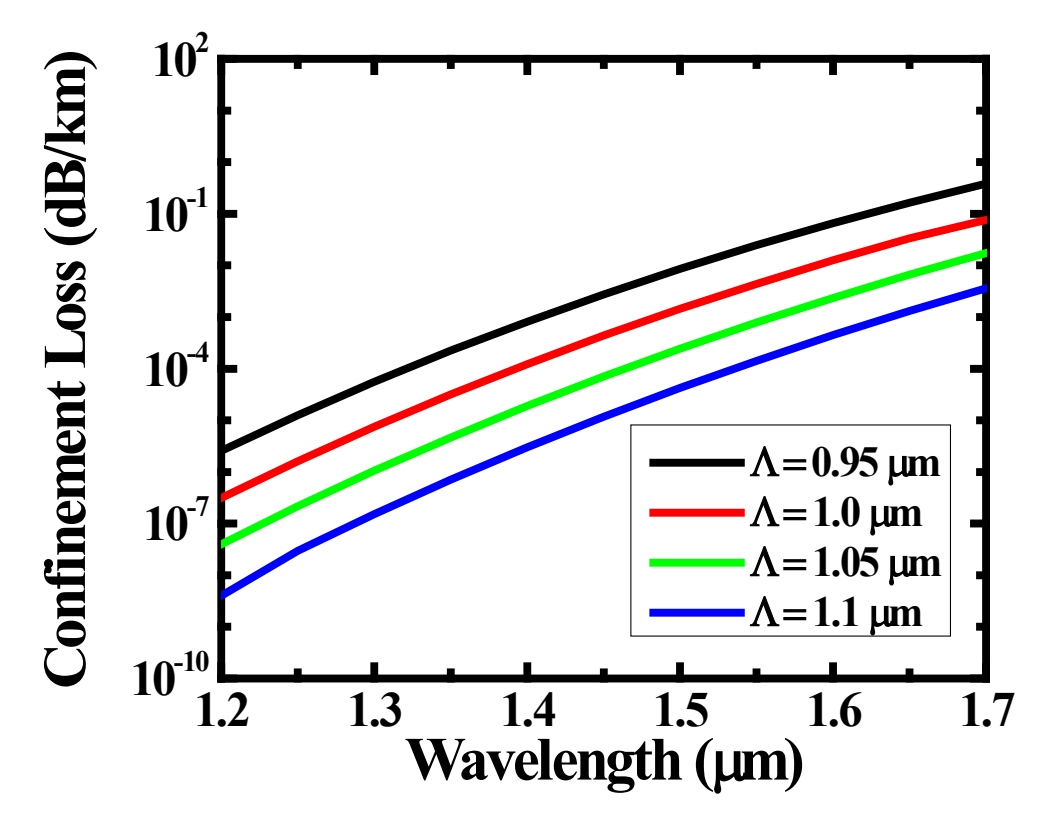
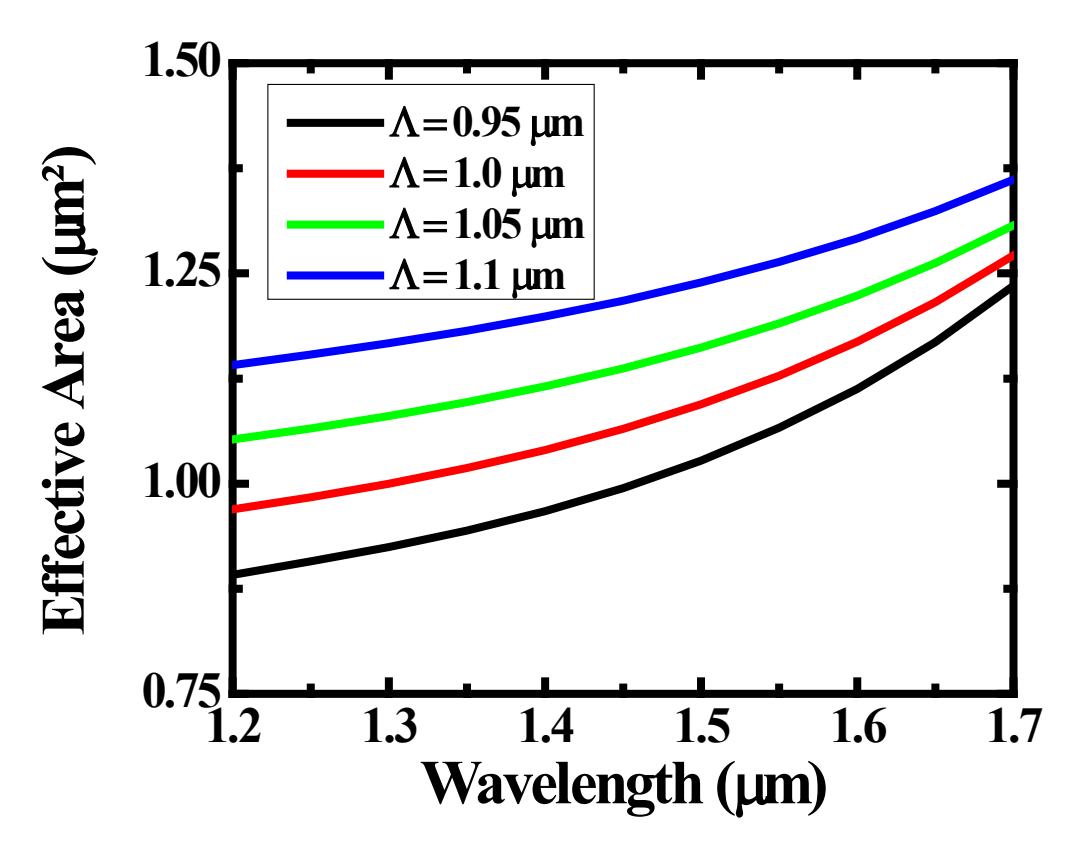


Figure 3: The effect of different values of  $\Lambda$  on the relationship between chromatic dispersion and wavelength.



**Figure 4:** The effect of different values of  $\Lambda$  on the relationship between confinement loss and wavelength.



**Figure 5:** The effect of different values of  $\Lambda$  on the relationship between effective area and wavelength.

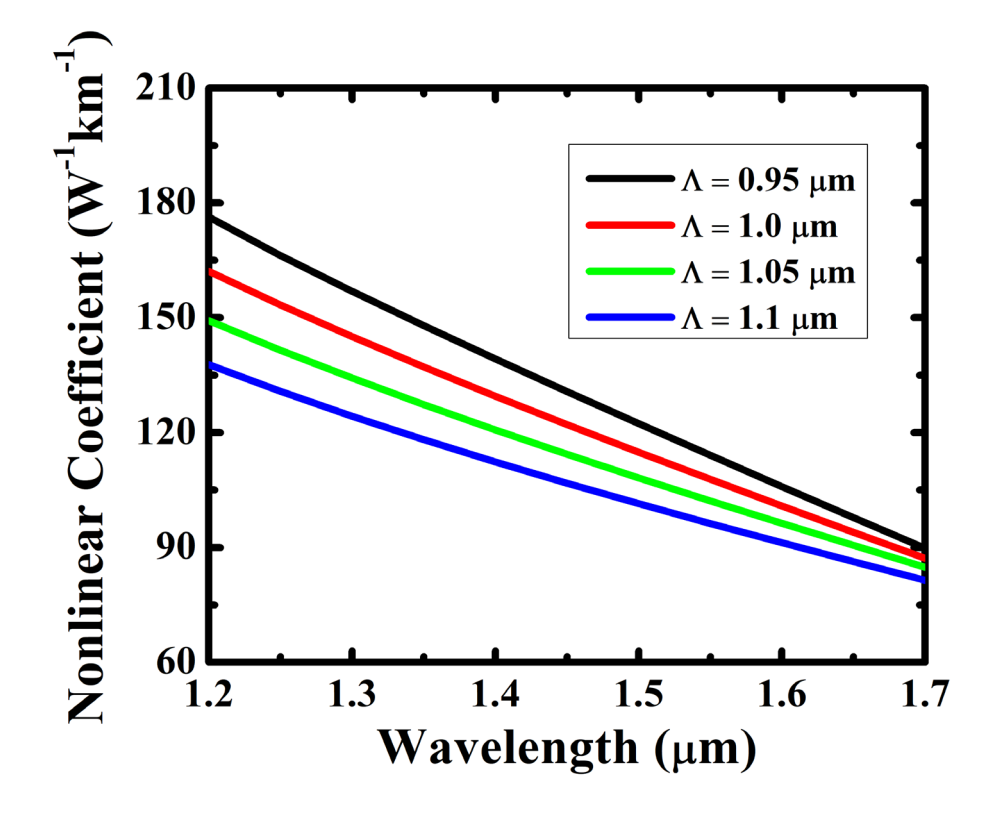


**Figure 6:** The effect of different values of  $\Lambda$  on the relationship between nonlinearity and wavelength.

Investigating confinement loss of PCF is crucial in determining light leakage from the core of PCF. Ideally, confinement loss needs to be kept as low as possible to prevent light leaking out from the core. Figure 4 illustrates the relationship between confinement loss and wavelength for different  $\Lambda$ . It can be seen that confinement loss increases with wavelength. Increasing  $\Lambda$ , however, results in lower confinement loss. With  $\Lambda$  = 1.1  $\mu$ m, confinement loss of 0.00014 dB/km is obtained, whilst  $\Lambda$  = 1.05  $\mu$ m and  $\Lambda$  = 1.0  $\mu$ m give confinement losses of 0.00078 dB/km and 0.0043 dB/km, respectively, at 1.55  $\mu$ m wavelength.

Effective area, Aeff and nonlinearity,  $\gamma$  are two other properties that need to be investigated to determine the applicability of the PCFs in nonlinear applications, such as in supercontinuum generation, which requires a high nonlinear coefficient. According to equation (6), the nonlinear coefficient,  $\gamma$  and effective area,  $A_{eff}$ , are inversely proportional to each other; with low  $A_{eff}$  resulting in a higher nonlinear coefficient,  $\gamma$ . This relationship is observed in Figures 5 and 6. It can be seen that the effective area,  $A_{eff}$ , increases with wavelength and  $\Lambda$ , whilst the nonlinear coefficient,  $\gamma$  decreases with both wavelength and  $\Lambda$ . With  $\Lambda = 1.0$  μm and  $\Lambda = 1.05$  μm, the effective area,  $A_{eff}$ , are 1.12 μm² and 1.19 μm², respectively, at 1.55 μm wavelength. Nonlinear coefficient,  $\gamma$  of 107.8 W<sup>-1</sup>km<sup>-1</sup> and 102.2 W<sup>-1</sup>km<sup>-1</sup> are obtained with  $\Lambda = 1.0$  μm and  $\Lambda = 1.05$  μm, respectively at 1.55 μm wavelength. At 1.55 μm wavelength,  $\Lambda = 0.95$  μm gives the lowest effective area,  $A_{eff}$  of 1.06 μm², which in turn gives the highest nonlinearity,  $\gamma$  of 114.0 W<sup>-1</sup>km<sup>-1</sup>. On the other hand,  $\Lambda = 1.1$  μm provides the highest  $A_{eff}$  of 1.26 μm² with the lowest nonlinear coefficient,  $\gamma$  value of 96.2 W<sup>-1</sup>km<sup>-1</sup> at 1.55 μm wavelength.

For the proposed PCF to be applicable as a dispersion compensating fibre (DCF) practically, the relative dispersion slope, RDS, of the proposed PCF has to match with RDS of single-mode fibre (SMF). It is given that RDS of a SMF is  $0.0036~\text{nm}^{-1}$  at  $1.55~\mu\text{m}$  wavelength; and as such, the RDS value of the proposed PCF needs to be as close as possible to  $0.0036~\text{nm}^{-1}$ , for the PCF to function as DCF. Via calculations, the RDS value close to  $0.0036~\text{nm}^{-1}$  at  $1.55~\mu\text{m}$  wavelength is only achieved with  $\Lambda = 1.0~\mu\text{m}$ , as depicted in Table 1. As such,  $\Lambda = 1.0~\mu\text{m}$  must be used for the proposed PCF to function as DCF; with the rest of the paper assuming this value of  $\Lambda$ . Fig. 7 shows RDS for different wavelengths with  $\Lambda = 1.0~\mu\text{m}$ .

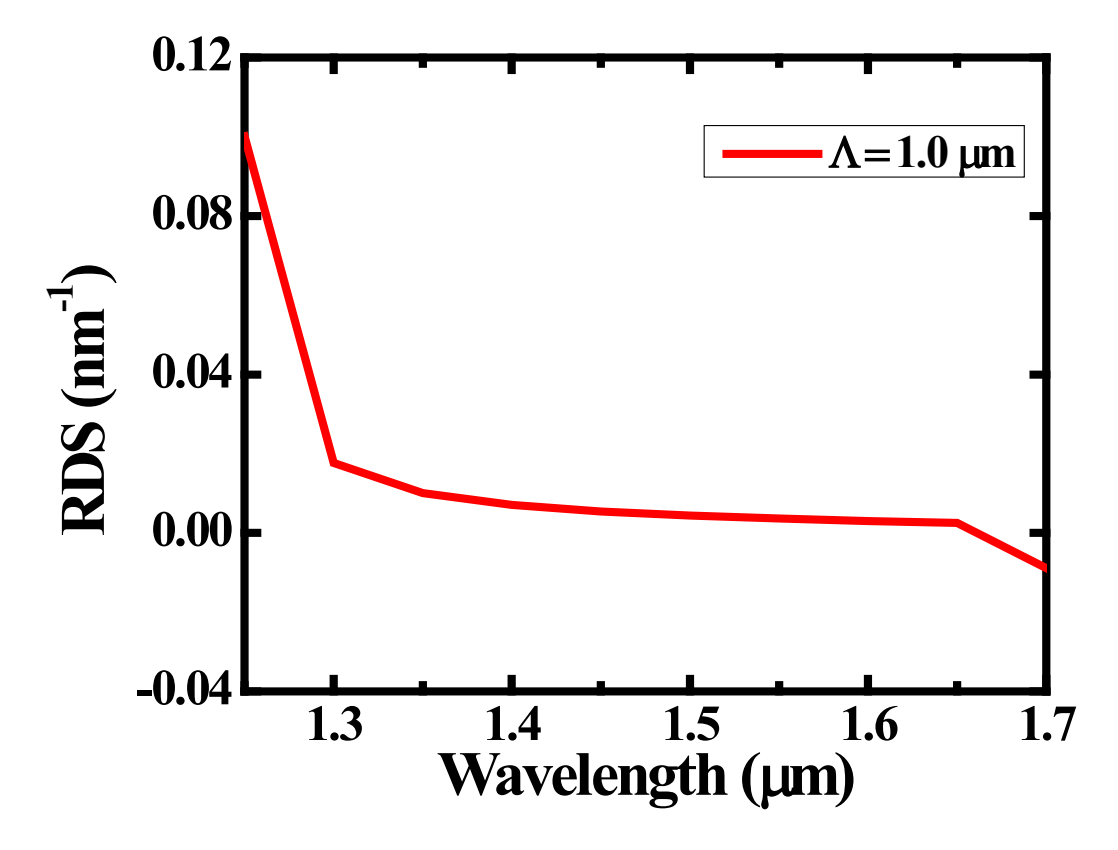


**Figure 7:** RDS of the optimum  $\Lambda$  value.

Table 1. The effect of changing  $\Lambda$  values on RDS of the fibre at 1.55  $\mu$ m wavelength.

Pitch, Λ (μm)	RDS (nm <sup>-1</sup> )
0.95	0.0028
1.0	0.0036
1.05	0.0047
1.1	0.0062

A high negative dispersion property is required for the PCF to compensate for the positive dispersion caused by the single-mode fibre. However, even after compensation, there still exists some leftover dispersion, widely known as total residual dispersion,  $D_T$ , which needs to be kept as low as possible. Therefore,  $D_T$  was also investigated in this study, and a graphical analysis of that property can be seen in Fig. 8. It can be seen that at 1.55  $\mu$ m, residual dispersion  $D_T$  approaches zero before it produces negative residual dispersion again. Based on this, the proposed PCF can cover a wide range of wavelengths, including the E+S+C+L+U transmission window wavelengths, with partial coverage of the O band (1320 - 1700 nm).

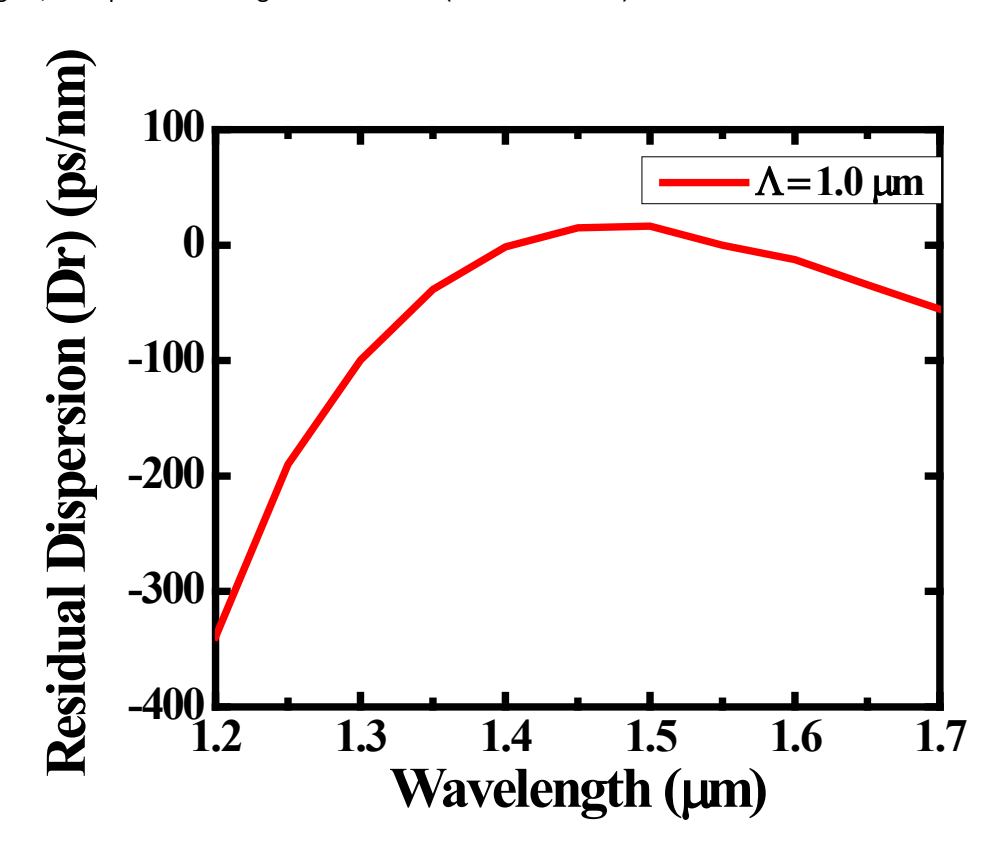


Figure 8. Residual Dispersion  $D_T$  of the optimum  $\Lambda$  value.

# 5.0 CONCLUSIONS

A PCF with 5 layers of square fillet air holes, based on an octagonal lattice design, has been proposed in this paper. The structure follows the golden ratio principle to give a strong but simple structure. Using the finite element method (FEM) and perfectly matched layer condition as boundary conditions, it has been shown that the proposed PCF yields high negative dispersion of -517 ps/(nm.km) at  $\Lambda = 0.95$   $\mu$ m and lowest confinement loss of 0.00014 dB/km, equivalent to the order of  $10^{-4}$  dB/km occurs at  $\Lambda = 1.1$   $\mu$ m. Both the highest and lowest dispersion occur at operating wavelength  $\lambda = 1.55$   $\mu$ m. Although it is ideal to have both high negative dispersion and low confinement loss in a PCF, results have shown that these are not attainable, with a trade-off between the two properties.

To further ascertain the suitability of the proposed PCF as a DCF, the residual dispersion slope RDS has been investigated. RDS value of  $0.0036~\text{nm}^{-1}$  occurs at  $\Lambda=1.0~\mu\text{m}$ , matching the RDS value of a single-mode fibre. Therefore,  $\Lambda=1.0~\mu\text{m}$  has been adopted for this proposed PCF. At this value of  $\Lambda$ , high negative dispersion of -377~ps/(nm.km) and low confinement loss of 0.0043~dB/km, in the order of  $10^{-3}~\text{dB/km}$ , are achieved. Additionally, an effective area of  $1.12~\mu\text{m}^{2}$ , which in turn gave a high nonlinear coefficient of  $107.8~\text{W}^{-1}\text{km}^{-1}$ , was found at the said optimum parameter. These show the suitability of the PCF for nonlinear applications, other than its application as a dispersion-compensating fibre. After analysing the total residual dispersion,  $D_T$ , it is found that the proposed PCF can cover the E+S+C+L+U wavelength bands, and a partial O band (1320 - 1700 nm), making it suitable as a wideband dispersion compensating fibre. Furthermore, because the PCF structure consists of similar air hole sizes and has a simple structure, the fabrication process of the PCF would be easier to establish.

#### References

- [1] J.C. Knight, *et al.*, "All-silica single-mode optical fiber with photonic crystal cladding," *Optics Letter*, vol. 21, pp. 1547–1549, Oct 1996.
- [2] P. St. J. Russell, "Photonic-Crystal Fibers," *Journal of Lightwave Technology*, vol. 24, pp. 4729-4749, Dec 2006.
- [3] K. Saitoh, and M. Koshiba, "Chromatic dispersion control in photonic crystal fibers: application to ultraflattened dispersion," *Optics Express*, vol. 11, pp. 843–852, Apr 2003.
- [4] L. Grüner-Nielsen, *et al.*, "Dispersion Compensating Fibers," *Journal of Lightwave Technology*, vol. 23, pp. 3566 3579, Nov 2005.
- [5] J.K. Ranka, *et al.*, "Visible continuum generation in air silica microstructure optical fibers with anomalous dispersion at 800 nm," *Optics Letter*, vol. 25, pp. 25–27, Jan 2000.
- [6] B. K. Paul, et al., "Design and analysis of slotted core photonic crystal fiber for gas sensing application," *Results in Physics*, vol.11, pp. 643–650, Dec 2018.
- [7] Y.S. Lee, *et al.*, "Dispersion compensating photonic crystal fiber using double-hole assisted core for high and uniform birefringence," *Optik*, vol. 147, pp. 334–342, Oct 2017.
- [8] M.R. Hasan, et al., "A single-mode highly birefringent dispersion- compensating photonic crystal fiber using hybrid cladding," *Journal of Modern Optics*, vol. 64, pp. 218-225, Aug 2016.
- [9] M. Faisal, et al., "Heptagonal Photonic Crystal Fiber for Dispersion Compensation with a Very Low Confinement Loss," 10th International Conference on Electrical and Computer Engineering (ICECE), 20-22 December 2018.
- [10] R. Ahmad, et al., "Modified Octagonal Photonic Crystal Fiber for Residual Dispersion Compensation over Telecommunication Bands," Radioengineering, vol. 27, pp. 10–15, Apr 2018.
- [11] A. Bala, et al., "Highly birefringent, highly negative dispersion compensating photonic crystal fiber," *Applied Optics*, vol. 56, pp. 7256-7261, Aug 2017.
- [12] G.B. Thapa and R. Thapa, "The Relation of Golden Ratio, Mathematics and Aesthetics," *Journal of the Institute of Engineering*, vol. 14, pp. 188–199, Feb 2018.
- [13] A. Rahman, et al., "Analysis of hexagonal photonic crystal fiber using the golden ratio," *International Journal of Engineering and Technology (UAE)*, vol. 7, Special Issue 13, pp. 5-7, July 2018.
- [14] A. Ferrando, *et al.*, "Full-vector analysis of a realistic photonic crystal fiber," *Optics Letters*, vol. 24, pp. 276-278, Apr 1999.
- [15] F. Begum, *et al.*, "Supercontinuum generation in square photonic crystal fiber with nearly zero ultraflattened chromatic dispersion and fabrication tolerance analysis," *Optics Communications*, vol. 284, pp. 965-970, Feb. 2011.
- [16] Agrawal, G.: 'Nonlinear Fiber Optics', 2nd ed.: Academic Press, San Diego, CA, 1995.
- [17] F. Begum and Pg E. Abas, "Near Infrared Supercontinuum Generation In Silica Based Photonic Crystal Fiber" *Progress In Electromagnetics Research C*, vol. 89, pp. 149-159, Jan 2019.
- [18] Md. R. Hasan, et al., "Tellurite glass defect-core spiral photonic crystal fiber with low loss and large negative flattened dispersion over S + C + L + U wavelength bands," Applied Optics, vol. 54, pp. 9456-9461, Nov 2015.
- [19] F. Begum, et al., "Novel Broadband Dispersion Compensating Photonic Crystal Fibers: Applications in High Speed Transmission Systems," *Optics & Laser Technology*, vol. 41, pp. 679-686, Sept. 2009.